AD-A041 599 AEROSPACE CORP EL SEGUNDO CALIF SPACE SCIENCES LAB F/G 4/1
CALCULATIONS OF SOFT AURORAL BREMSSTRAHLUNG AND K ALPHA LINE EM--ETC(U)
JUN 77 J G LUHMANN, J B BLAKE F04701-76-C-0077
UNCLASSIFIED TR-0077(2260-20)-8 SAMSO-TR-77-126 NL

| OF |
AD
A041599

END

DATE
FILMED
8-77

REPORT SAMSO-TR-77-126

Calculations of Soft Auroral Bremsstrahlung and K_α Line Emission at Satellite Altitude

Space Sciences Laboratory
The Ivan A. Getting Laboratories
The Aerospace Corporation
El Segundo, Calif. 90245

23 June 1977

Interim Report

Prepared for

SPACE AND MISSILE SYSTEMS ORGANIZATION
AIR FORCE SYSTEMS COMMAND
Los Angeles Air Force Station
P.O. Box 92960, Worldway Postal Center
Los Angeles, Calif. 90009

This report was submitted by The Aerospace Corporation, El Segundo, CA 90245, under Contract F04701-76-C-0077 with the Space and Missile Systems Organization, Deputy for Advanced Space Programs, P.O. Box 92960, Worldway Postal Center, Los Angeles, CA 90009. It was reviewed and approved for The Aerospace Corporation by G. A. Paulikas, Director, Space Sciences Laboratory. Lieutenant Dara Batki, SAMSO/YAPT, was the Project Officer for Advanced Space Programs.

This report has been reviewed by the Information Office (OI) and is releasable to the National Technical Information Service (NTIS). At NTIS, it will be available to the general public, including foreign nations.

This technical report has been reviewed and is approved for publication. Publication of this report does not constitute Air Force approval of the report's findings or conclusions. It is published only for the exchange and stimulation of ideas.

Dara Batki

Dara Batki, Lt, USAF
Project Officer

J Gassmann

Joseph Gassmann, Major, USAF

FOR THE COMMANDER

Leonard E. Baltzell

LEONARD E. BALTZELL, Colonel, USAF
Assistant Deputy for Advanced Space Programs

UNCLASSIFIED

SECURITY CLASSIFICATION OF THIS PAGE *(When Data Entered)*

REPORT DOCUMENTATION PAGE		READ INSTRUCTIONS BEFORE COMPLETING FORM
1. REPORT NUMBER SAMSO-TR-77-126	2. GOVT ACCESSION NO.	3. RECIPIENT'S CATALOG NUMBER
4. TITLE *(and Subtitle)* CALCULATIONS OF SOFT AURORAL BREMSSTRAHLUNG AND K_α LINE EMISSION AT SATELLITE ALTITUDE		5. TYPE OF REPORT & PERIOD COVERED Interim rept.
		6. PERFORMING ORG. REPORT NUMBER TR-0077(2260-20)-8
7. AUTHOR(s) Janet G. Luhmann and J. Bernard Blake		8. CONTRACT OR GRANT NUMBER(s) F04701-76-C-0077
9. PERFORMING ORGANIZATION NAME AND ADDRESS The Aerospace Corporation El Segundo, Calif. 90245		10. PROGRAM ELEMENT, PROJECT, TASK AREA & WORK UNIT NUMBERS 31p.
11. CONTROLLING OFFICE NAME AND ADDRESS Space and Missile Systems Organization Air Force Systems Command Los Angeles, Calif. 90009		12. REPORT DATE 23 June 1977 13. NUMBER OF PAGES 27
14. MONITORING AGENCY NAME & ADDRESS *(if different from Controlling Office)*		15. SECURITY CLASS. *(of this report)* Unclassified 15a. DECLASSIFICATION/DOWNGRADING SCHEDULE

16. DISTRIBUTION STATEMENT *(of this Report)*

Approved for public release; distribution unlimited.

17. DISTRIBUTION STATEMENT *(of the abstract entered in Block 20, if different from Report)*

18. SUPPLEMENTARY NOTES

19. KEY WORDS *(Continue on reverse side if necessary and identify by block number)*

Auroral X-Rays

20. ABSTRACT *(Continue on reverse side if necessary and identify by block number)*

Satellite altitude (450 nm) fluxes of 0.1- to 10-KeV auroral x-rays are calculated for some typical forms of incident electron spectra. Both bremsstrahlung and K_α line emission are included. These calculations indicate that K_α emission can increase the observable intensity of satellite altitude auroral x-rays by up to 100 times, thereby making soft x-rays an ideal medium for imaging the aurora.

DD FORM 1473 (FACSIMILE)

UNCLASSIFIED

SECURITY CLASSIFICATION OF THIS PAGE *(When Data Entered)*

CONTENTS

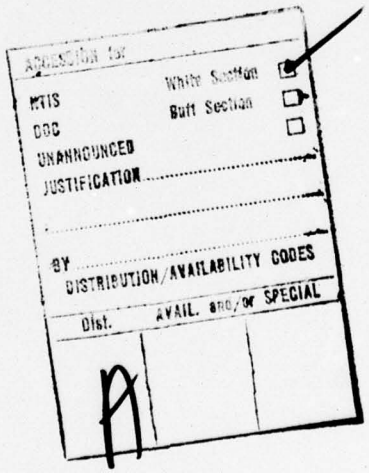

FIGURES

I. INTRODUCTION

Observations of the auroral morphology from space have been carried out recently with both the line-scanning radiometers aboard the DMSP meterological satellites [cf. Rogers et al., (1974); Snyder et al., (1974); Mizera et al., (1975)] and the auroral scanners aboard the ISIS-2 spacecraft (Lui and Anger, 1973; Lui et al., 1975). These data, which provide a global view, have opened a new era in the study of the aurora. In general, the current satellite-borne instruments respond to visible and near-visible atomic and molecular line emissions that result from collisional excitation of the atmospheric constituents by the auroral particles (cf. Jones, 1974). The DMSP sensor responds to light in the 6000 Å to 10000 Å (FWHM) region; the ISIS-2 sensors observe the 5577 Å and 6300 Å lines of atomic oxygen and the 3914 Å line of molecular nitrogen. However, optical imaging of the aurora suffers from several limitations. For example, since optical imaging requires a dark earth, sunlight and even moonlight prohibits observations. Also, the optical emissions are related to the input auroral electrons in a complex fashion dependent upon the details of atmospheric chemical processes and thus are not directly interpretable in terms of the energy input of the precipitating electrons (Jones, 1974). Furthermore, the precipitation of very energetic electrons, which occurs at subauroral latitudes (Potemra and Zmuda, 1970, Torr, et al., 1975) is not seen at all in the visible wavelengths. In view of these limitations, a global picture of electron precipitation using x-ray wavelengths would be valuable.

Observations of x-rays at balloon altitude from precipitating particles have been carried out for some time (cf. Anderson, 1965; Kremser, 1967). The low energy threshold of such measurements is of the order of 20 keV because the atmosphere absorbs softer photons between the balloon and the source region. This cutoff restricts the observations to energetic precipitation events. In order to observe typical auroral precipitation, it is necessary to detect x-rays in the keV energy range and below. These soft auroral x-rays reach satellite altitudes where they can be detected using techniques developed for x-ray astronomy (cf. Peterson, 1975). Satellite observations of x-rays generated by precipitating electrons have already been reported by Imhof (1975) and Imhof et al. (1974), 1975a), 1975b). However, these data were obtained with a Ge(Li) spectrometer with a lower threshold of ~50 keV. In this paper we present calculations of the low-energy satellite-altitude auroral x-ray spectra that result from some typical electron influxes. The results of these calculations provide an estimate of the soft x-ray flux that is incident on satellite borne detectors which are exposed to the auroral atmosphere.

The most familiar mechanism of auroral x-ray production is the bremsstrahlung process (Rees, 1964; Berger and Seltzer, 1972; Vij and Venkatesan, 1975). At satellite altitudes, bremsstrahlung spectra above ~10 keV are expected to exhibit power law forms with spectral indices that depend on the hardness of the precipitating electrons (Seltzer and Berger, 1974). Below 10 keV the bremsstrahlung spectra peak at an

energy that is determined by both the incident electron spectrum and the atmospheric attenuation coefficients, and then fall rapidly toward zero. Attenuation is largely determined by the major constituents, nitrogen and oxygen. The absorption cross-sections for these elements are given by Hubbell (1971).

In addition to bremsstrahlung, K-shell line emission contributes to the auroral x-ray flux at several discrete energies. (Kraushaar, 1974). The most important atmospheric emitters of K-shell x-rays are nitrogen, oxygen and argon. These atoms emit K_α photons at 0.396 keV, 0.525 keV and 2.96 keV, respectively. In Figure 1, the measured K_α cross sections of nitrogen, oxygen and argon atoms over a range of incident electron energies (Tawara et al., 1973) are compared with the bremsstrahlung cross-section for the emission of a photon in the 400 eV to 500 eV energy range. Because the line emission is discrete whereas bremsstrahlung is a continuum, the determination of the relative signal strengths in a sensor depends upon its energy passband. A nominal value of 100 eV was selected for this comparison. The cross-section data shown in Figure 1 indicate that line emission will be a major source of x-ray photons at low energy. In addition to serving as a major source of x-rays for remote sensing of auroral precipitation by satellite, K_α emission provides a signature which identifies x-rays of auroral origin. This characteristic could be of great value to x-ray astronomers who must substract atmospheric backgrounds from their balloon and rocket-based observations of galactic x-rays. The K_α emission also provides a means

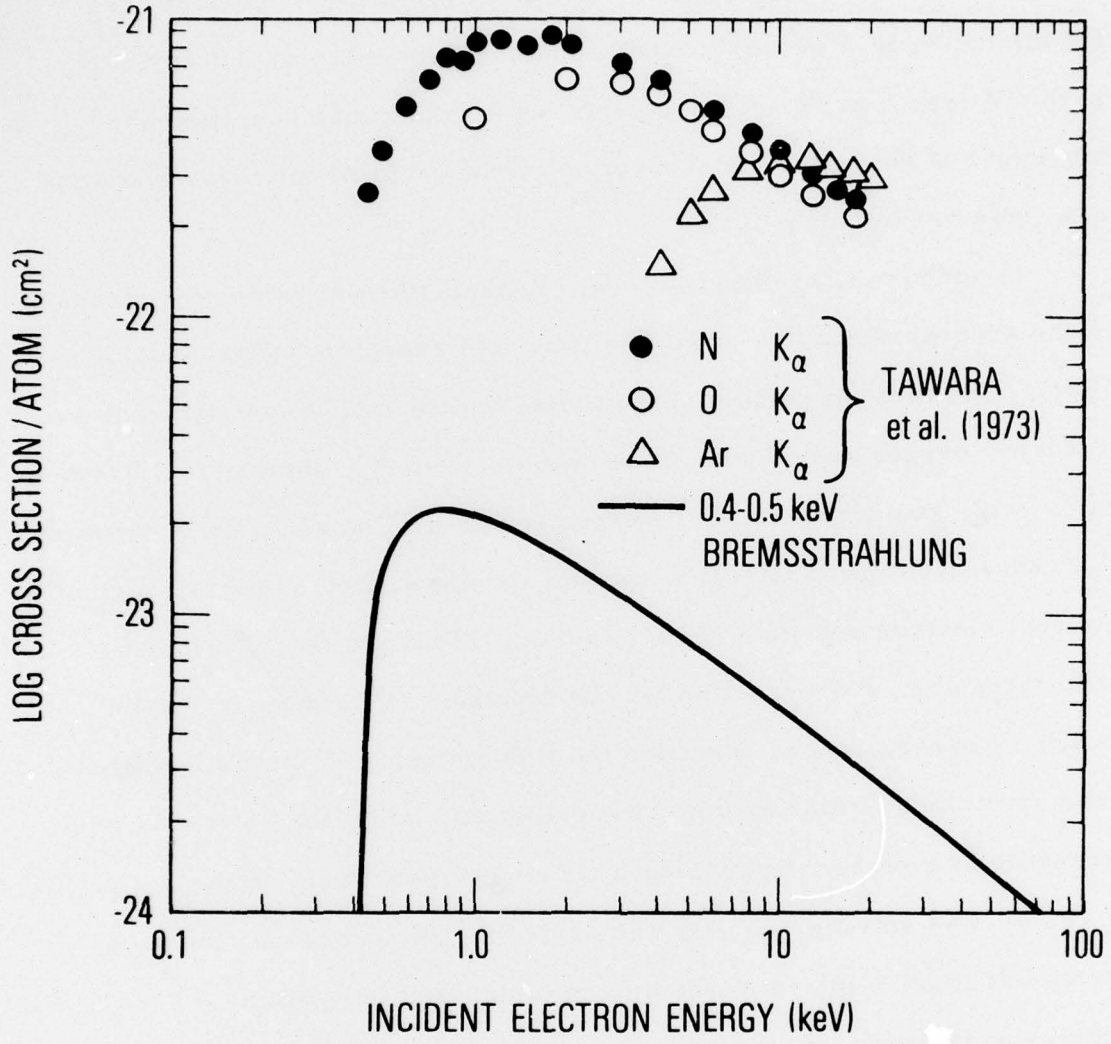

Figure 1. Production Cross Sections for Nitrogen, Oxygen, and Argon K_α Emission as Measured by Tawara et al. (1973). The cross section for bremsstrahlung emission in the 0.4- to 0.5-keV band is shown for comparison.

of remotely sensing electron precipitation in other planetary atmospheres, while yielding information about the atmospheric composition.

This paper describes some calculations of the upward directed x-ray flux resulting from electron precipitation at a typical satellite altitude of 450 nm. Both bremsstrahlung and line emission are considered. Emphasis is placed on energies between 100 eV and 10 keV. The upward-directed x-ray fluxes are calculated for a plane-parallel atmosphere excited by auroral electrons with exponential energy spectra. A more realistic case of an emitting auroral arc below the satellite also is considered for the same incident electron spectra. The calculational procedure then is applied to the analysis of some previously reported auroral x-ray and electron data.

II. DESCRIPTION OF THE CALCULATIONS

A. Emission from a Plane Parallel Atmosphere

A procedure has been developed (Luhmann, 1976a) for predicting the bremsstrahlung spectrum at any atmospheric depth given an arbitrary electron spectrum incident on a plane parallel atmosphere. A Fokker-Planck equation that describes electron penetration into the atmosphere was solved analytically for the case of widespread stable precipitation without magnetic mirroring (Luhmann, 1976b). The solution gives the electron spectrum as a function of altitude as determined by ionization loss. With the aid of a standard numerical integration technique, the local volume emissivity of x-rays is computed from the local electron spectrum and the cross section for x-ray emission. An additional integral describing the radiative transfer of these x-rays in the atmosphere then provides the bremsstrahlung intensity at a given altitude. The hemispherical flux is obtained by integrating the intensity over upward or downward directed photon angles.

The adaptation of the bremsstrahlung calculational procedure to line emission is straightforward. The upward directed bremsstrahlung flux at atmospheric depth X and photon energy k, as seen by a satellite with a downward-looking hemispherical detector, is given by (Luhmann, 1976a).

$$\Phi_{up}(X, k) = \int_{\pi/2}^{\pi} d\eta \mathcal{I}_{up} \qquad (1)$$

Here $\mathcal{I}_{up}$ is the intensity in photons/(cm^2-sec-keV) which is related to the Bethe-Heitler cross section for bremsstrahlung emission $d\sigma_B/dk$ through the formula

$$\mathcal{I}_{up} = \int_0^{(1030 - X)\sec\eta} P_B \exp\left(-\mu_a |X - x| \sec\eta\right) dx \sec\eta \qquad (2)$$

where

$$P_B(X, k, \eta) =$$

$$\frac{1}{M} \int_k^\infty dT \left\{ \frac{d\sigma_B}{dk} \int_0^1 d\mu \int_0^{2\pi} d\tau \, \frac{v}{2\pi} f(\mu, x, T)\, \omega(\mu, \eta, \tau) \right\} \qquad (3)$$

The integral P_B is the volume emissivity for bremsstrahlung. Other quantities that appear above are the photon direction angle η, the mass absorption coefficient for air μ_a, the atmospheric depth in g-cm^{-2} x, the mean atomic weight of the atmospheric constituents M, the electron kinetic energy T, the electron velocity v, the electron zenith-angle cosine μ, the photon azimuth τ, and the angular distribution of the bremsstrahlung, $\omega(\mu, \eta, \tau)$. Figure 2 illustrates the geometric relationship between the angles η and τ. The function $f(\mu, x, T)$ is the electron distribution derived by Luhmann (1976b). The Compton cross-section was set equal to zero in the formulation of the x-ray flux integral (1). This approximation is valid at the low energies of interest because the Compton cross-section is very small relative to the photoelectric cross-section for few keV photons in air. In order to obtain Φ_{up} for a line, equation (3)

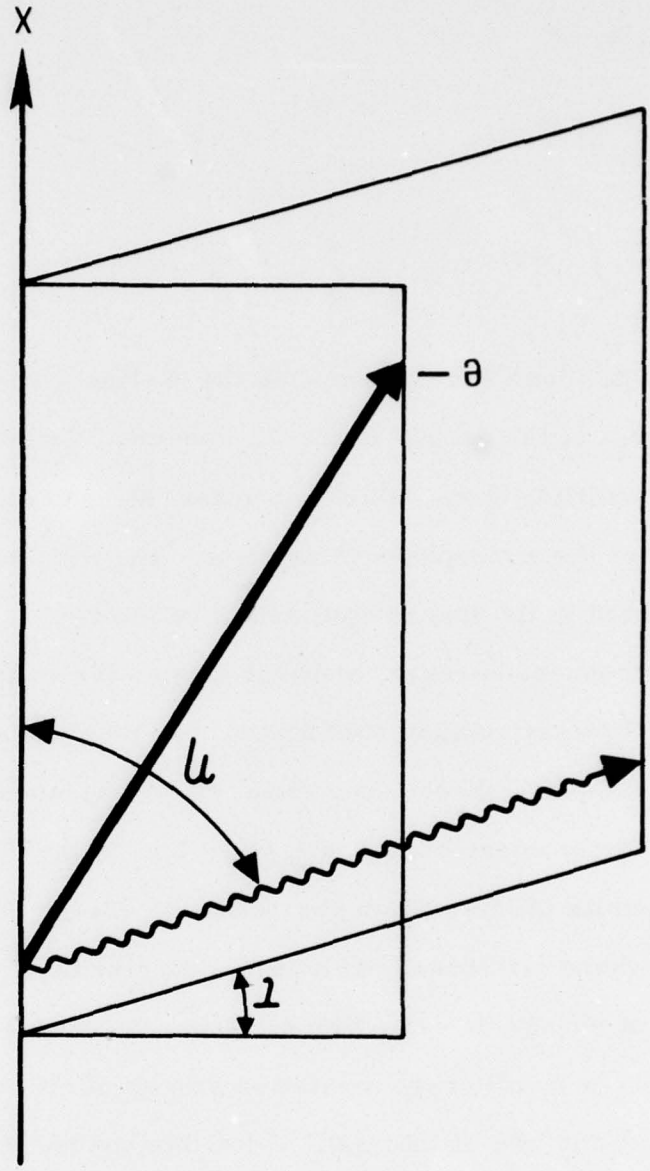

Figure 2. Geometry of Photon Emission With Respect to the Electron Velocity Vector, Showing Orientation of the Photon Direction Angle η and the Azimuth τ

for the volume emissivity is restated in terms of the cross-section for line emission $\sigma_K(T)$:

$$P_K(x, k_K, \eta) =$$

$$\frac{x_j}{x M_j} \int_{E_K}^{\infty} dT \quad \frac{\sigma_{K_j}(T)}{\Delta} \int_0^1 d\mu \; \frac{v}{\pi} \; f(\mu, x, T) \qquad (4)$$

The subscript K identifies the above as the K-line emissivity. In equation (4), k_K is the energy of the K_α photon. Subscript j denotes the species of emitting atom, which has mass M_j and constitutes a fraction x_j/x of the atmosphere at depth x. The angular distribution of photons emitted in the line is assumed to be isotropic. The quantity Δ(in keV) is introduced because, although line emission is discrete (in contrast to the bremsstrahlung continuum), one must consider the finite passband of a detector. Hence, the ratio σ_K/Δ replaces the differential cross-section for bremsstrahlung $d\sigma_B/dk$. One further modification is needed in the limits of integration over electron energy T. For bremsstrahlung, only those electrons with kinetic energies of k or greater can yield a photon of energy k. For line emission the cross-sections have a sharp low energy cutoff at the excitation energy of the K shell E_K, corresponding to the line of interest. Once this change in the calculation of the emissivity is effected, the calculation of Φ_{up} for the line proceeds through the integrals (1) and (2) as in the bremsstrahlung flux calculation with P_K replacing P_B. The numerical evaluation of equations (1) - (4)

provides estimates of the bremsstrahlung and K_α line fluxes from a plane-parallel emitting atmosphere viewed by a downward-looking hemispherical detector.

B. Finite Aurora Correction

Because auroral emission is generally confined to a limited region of the atmosphere as seen from a satellite, a method for estimating the x-ray flux from an arc-like structure is desirable. An approximate correction to the infinite aurora calculation can be incorporated simply if it is assumed that only the primary unscattered K_α photons are important. The geometry is illustrated in Figure 3a. If the detector is situated above the midpoint of the long axis of the arc, as shown here, the finite aurora geometry can be included merely by restricting the angular integration over τ and η in equations (1) - (3). A corresponding angular correction factor must be applied to equation (4). Figure 3b illustrates how different τ intervals can be specified for each direction angle η in each of the numerical integration steps. This method of correction actually restricts the angles from which photons can arrive at the detector at the origin. In contrast, all τ and η are covered by the integration in the infinite aurora case.

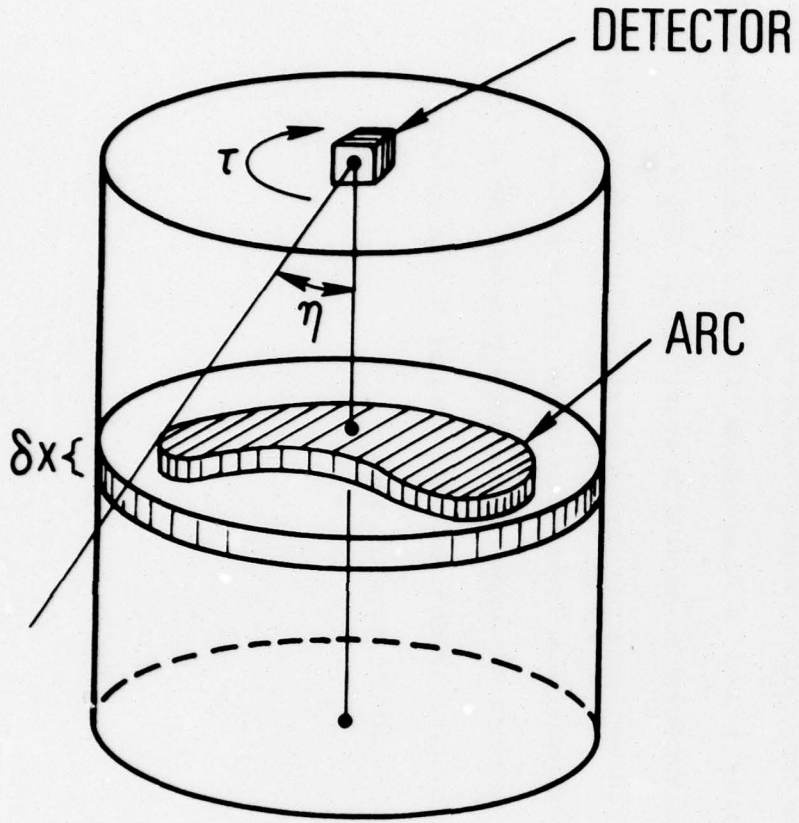

Figure 3(a). Geometry Assumed in Finite Aurora Correction. Photons from an emitting layer of the atmosphere δx can reach the detector only if their direction angles η and τ lie in a restricted range.

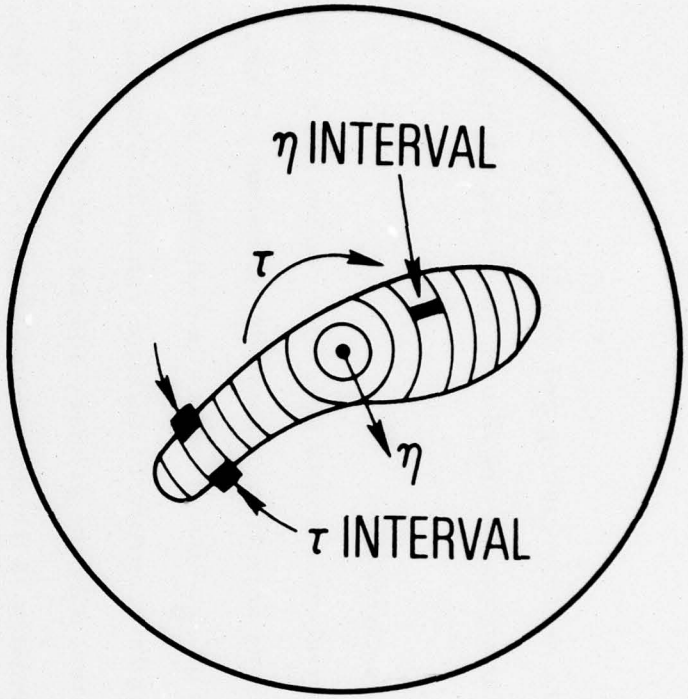

Figure 3(b). Division of the Arc, as Seen by the Detector, Into η and τ Integration Intervals

III. RESULTS

A. Exponential Electron Spectra

Figure 4 illustrates some bremsstrahlung spectra that were calculated from equations (1) - (3) assuming normalized exponential electron spectra incident on a plane-parallel atmosphere. These results represent the observed spectrum at 450 nm for e-folding energies α of 1, 5, 10, 15 and 30 keV. The inset, which is a magnification of the low-energy spectrum for α equal to 1 keV and 15 keV, shows the structure that is introduced by the K absorption edges of nitrogen and oxygen. The corresponding results from the Monte Carlo calculations of Seltzer and Berger (1974), which do not extend below 10 keV, compare favorably with the present calculation at higher energies.

The K_α line fluxes for the same case of a parallel atmosphere and exponential electron spectra were obtained from equation (4). In computing the line fluxes, the fractional contributions x_j/x of each constituent to the atmosphere were derived from the Jacchia model atmosphere (Jacchia, 1971). In all calculations of the line flux a nominal value of 100 eV was adopted for the quantity Δ which appears in equation (4). This is a typical value for the resolution (FWHM) at 5.9 keV of commercially available x-ray detector systems employing Si(Li) sensor elements. The meaning of a constant Δ is that the detectors have a rectangular energy response, 100 eV wide, centered on the lines of interest.

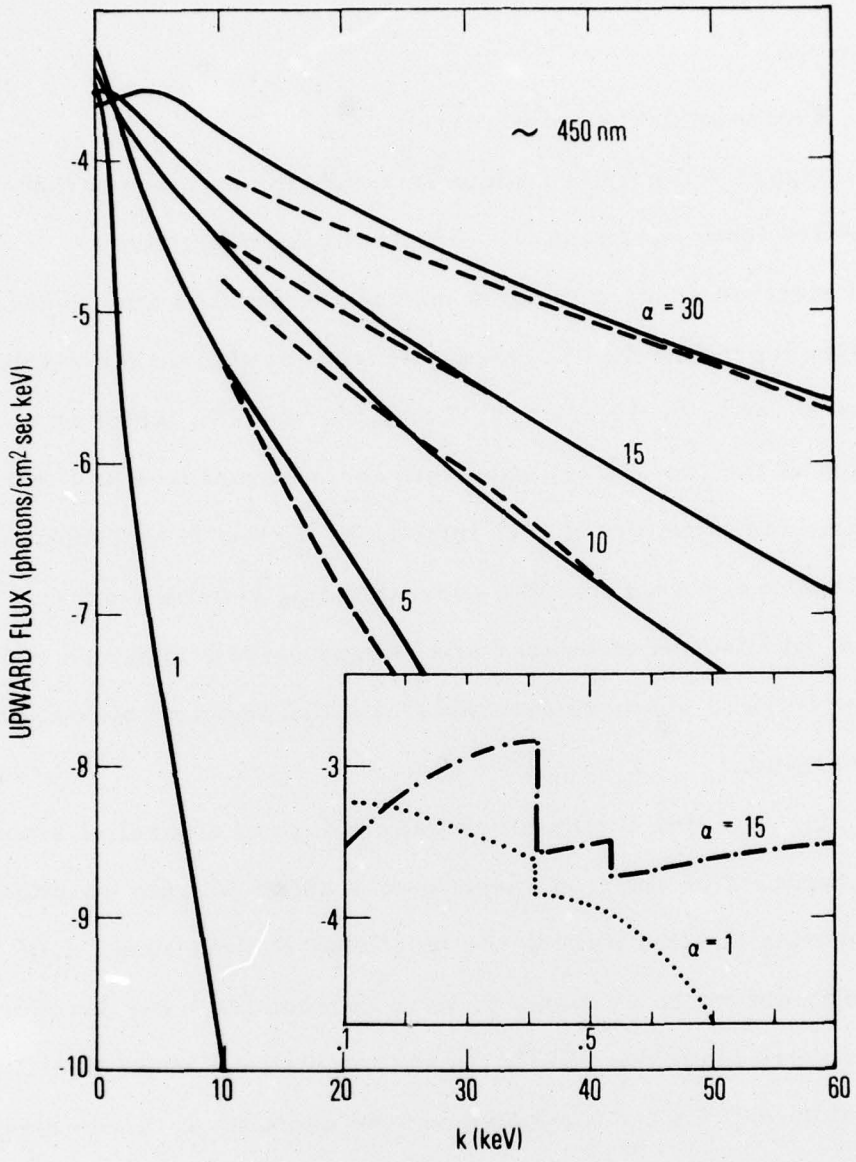

Figure 4. Upward Directed Flux Spectra of Bremsstrahlung X-Rays From a Plane Parallel Atmosphere Generated by Incident Exponential Electron Spectra With Various e-Folding Energies α. The corresponding Monte Carlo results from Seltzer and Berger (1974) are shown by the dashed lines. The inset shows the structure in the low-energy spectrum that is produced by the K absorption edges of nitrogen and oxygen.

Figure 5 shows how the ratio of line flux to bremsstrahlung flux within the energy bands shown varies with the e-folding energy α for a plane-parallel atmosphere. As expected from the comparison of cross-sections that was given in Figure 2, the nitrogen and oxygen K_α line intensity dominates the bremsstrahlung continuum. Both oxygen and nitrogen ratios reach a maximum at $\alpha \approx 10$ keV because the integral in equation (4) is a maximum near this value for the normalized exponential electron spectra considered here. The results shown in Figure 4 indicate that the .4 - .5 keV bremsstrahlung flux does not vary greatly with α. Variations in the line emission thus determine the variation in the flux ratios shown in Figure 5.

Figure 6 illustrates the effect that the finite aurora correction has on the line to bremsstrahlung flux ratios. In this example, the geometric model for the x-ray emitting arc was derived from an all-sky photograph reported by Wilson et al. (1969). The inset shows the assumed geometry of the emitting region as seen from the satellite. The intensity ratios calculated for this arc differ from those in Figure 5 because of the different angular distributions of the bremsstrahlung and line emission. Figures 5 and 6 together indicate the order of magnitude of the possible intensity ratios. Most importantly, these results suggest that K_α line emission can intensify the auroral x-ray flux by 30 to 100 times in selected energy windows of several hundred eV widths.

B. Application to Observations

With few exceptions, past experiments have provided either

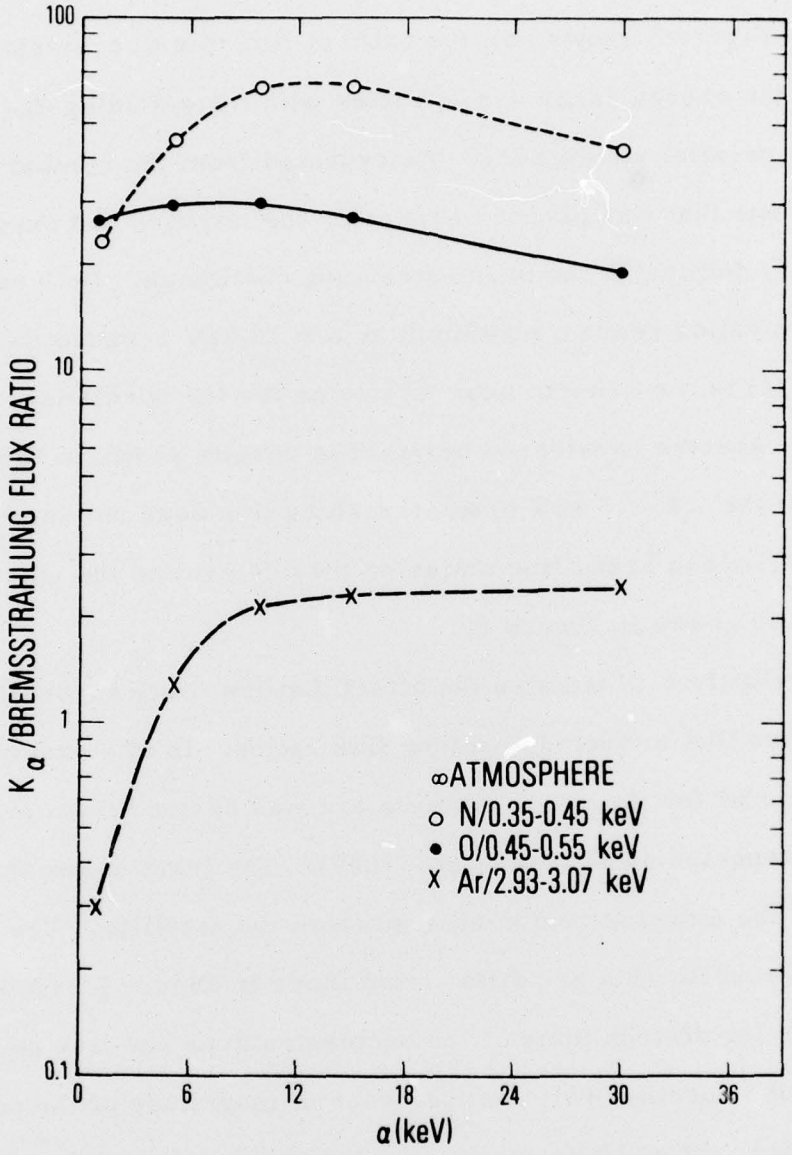

Figure 5. Ratio of K_α Line Emission to Bremsstrahlung Emission in the 100-eV Band Centered on the Line Versus the e-Folding Energy of the Incident Electron Spectrum for a Plane Parallel Emitting Atmosphere

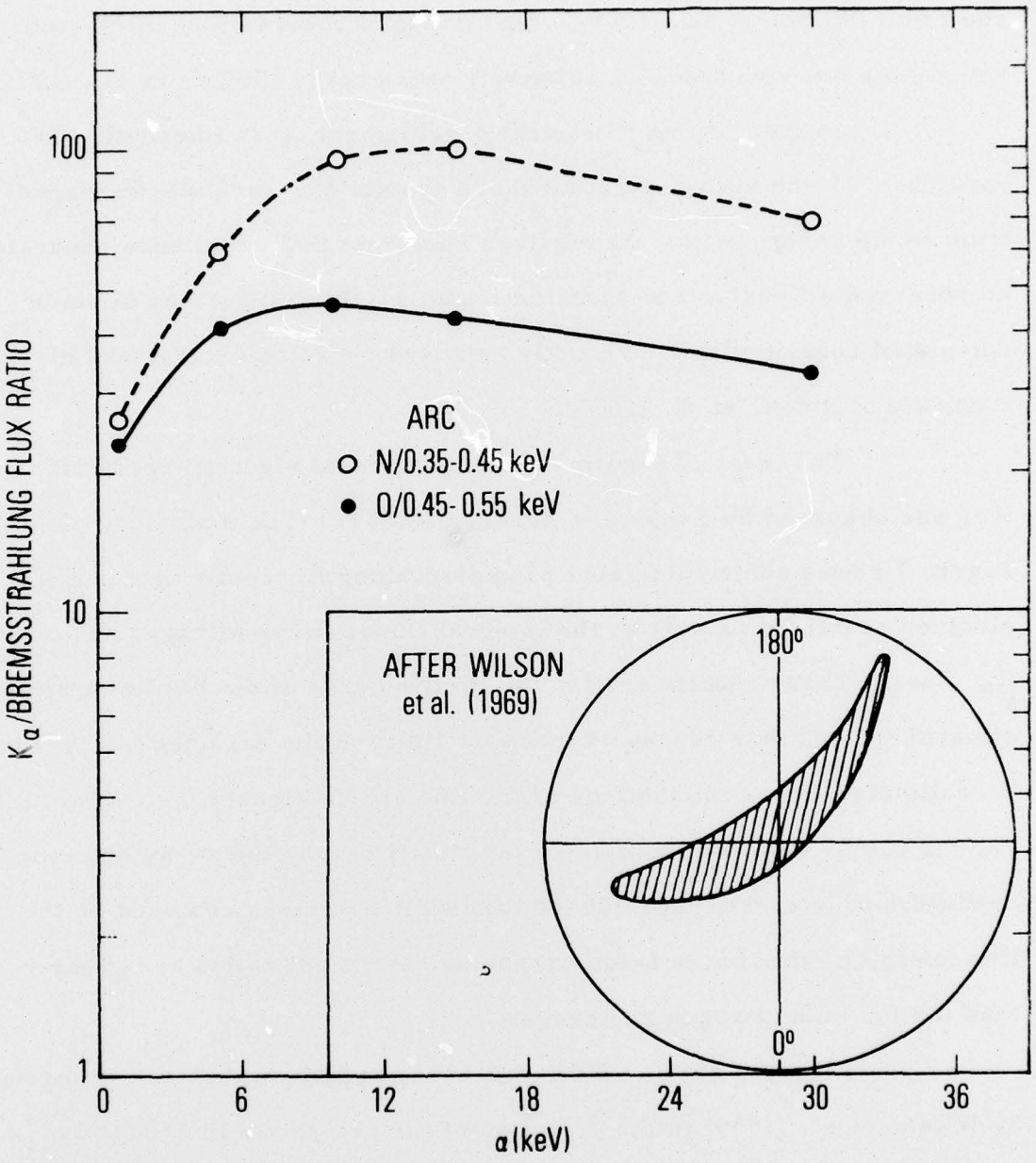

Figure 6. Same as Figure 5 but With the Finite Aurora Correction Incorporated. The assumed geometry of the arc is shown in the inset.

an auroral electron spectrum (Frank and Ackerson, 1971) or an x-ray spectrum (Wilson et al., 1969). Simultaneous observations of electrons and x-rays are recent and at relatively high energy (Imhof, et al., 1974).

In view of this historical development, it is interesting to consider: 1) the x-ray spectrum that a typical observed electron spectrum would generate; 2) the electron spectrum that could have generated an observed auroral x-ray spectrum, and 3) the comparison of some calculated results with the recently reported correlated x-ray and electron data of Imhof, et al. (1974).

The inset of Figure 7 gives an auroral electron spectrum that was observed by Frank and Ackerson (1971). The main body of Figure 7 shows some calculated bremsstrahlung fluxes for this incident electron spectrum as well as the integral fluxes in the nitrogen and oxygen K_α lines. These results are for the limiting case of an infinite emitting atmosphere and thus represent an upper limit on the expected x-ray flux. An estimate of the contributions of the line and continuum fluxes to observations can be obtained by dividing the line fluxes by the x-ray detector bandwidth of interest. For 100 eV bandwidth detectors centered on the line energies, the line to bremsstrahlung continuum ratios are greater than ten for both nitrogen and oxygen.

Figure 8 shows an auroral x-ray spectrum that was observed by Wilson et al. (1969) in the direction of the arc shown in Figure 6. These observations did not include the energy range of the K_α lines. The solid line is the result of a calculation by the present method for an incident

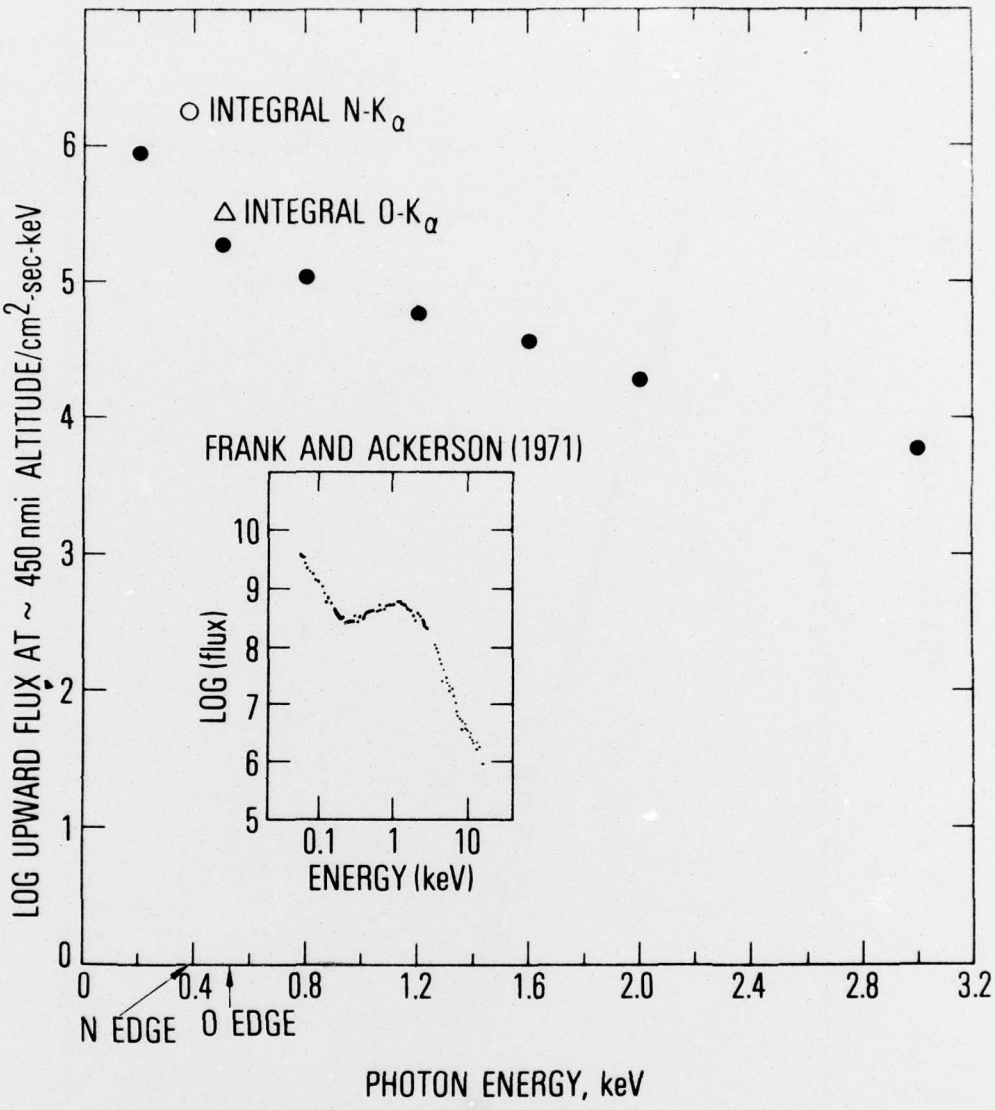

Figure 7. Predicted Low-Energy X-Ray Spectrum for the Incident Electron Spectrum Shown in the Inset. Black points indicate differential bremsstrahlung fluxes. White points give the integral K_α line fluxes from nitrogen and oxygen.

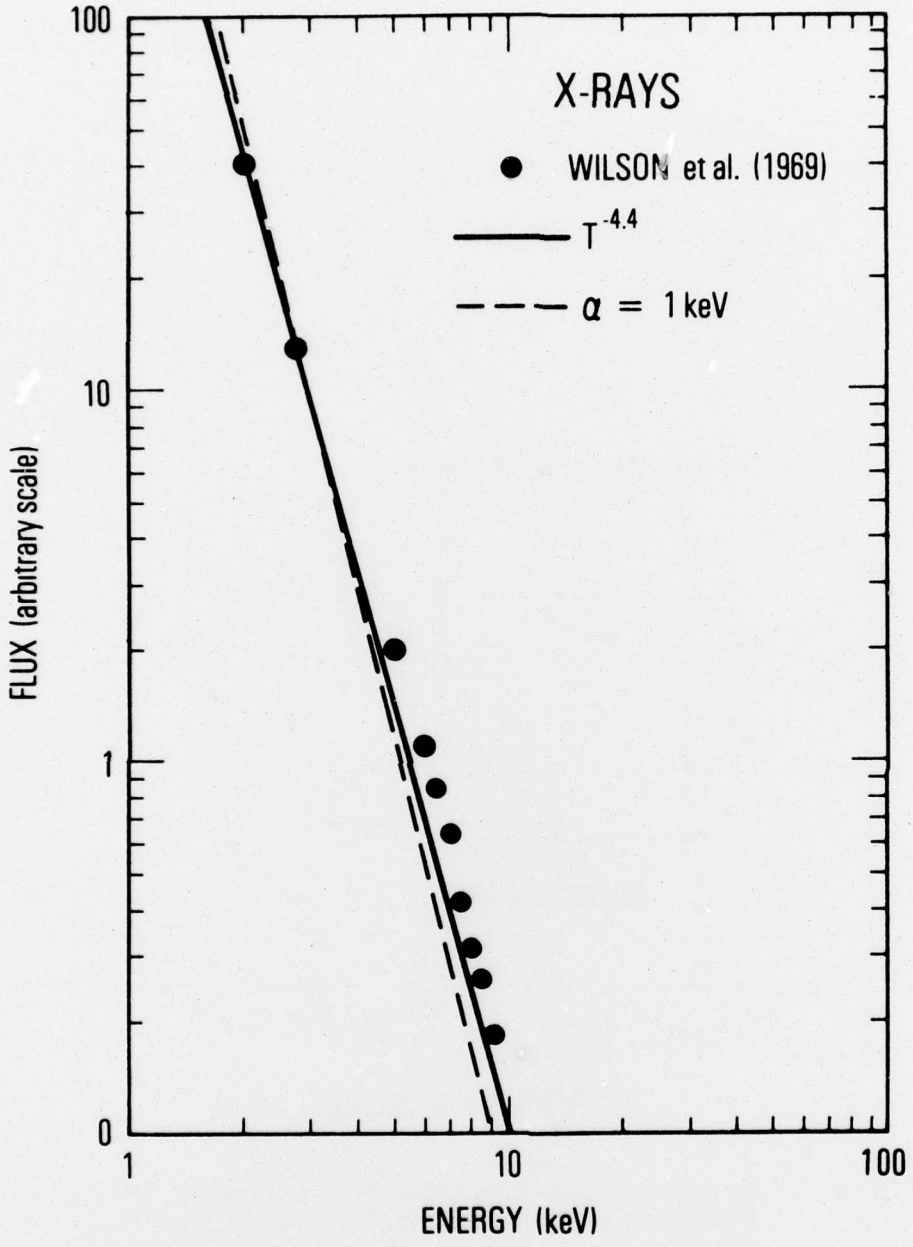

Figure 8. X-Ray Data From Wilson et al. (1969) Compared With Calculated Bremsstrahlung Spectra for Several Forms of Incident Electron Spectrum

power-law electron spectrum with a spectral index of -4.4. This electron spectrum, which was suggested by Wilson et al., (1969) apparently provides an x-ray spectrum that is consistent with the observations. However, as shown by the dashed line, the x-rays generated by the exponential electron spectrum with α = 1 keV also reasonably fits the data. This example illustrates how the inference of an auroral electron spectrum from x-ray data can be somewhat ambiguous.

Imhof et al. (1974) reported correlated electron and x-ray data. The observed x-ray fluxes were compared with a spectrum calculated from the measured electron fluxes using a Monte Carlo technique. For comparison, this same procedure was carried out using the present calculational method. Figure 9 shows the data reported by Imhof et al. (1974) together with the reults of the present calculation. The x-ray spectrum obtained for the observed electron spectrum from equations (1) - (3) is indicated by the solid line. The normalization is arbitrary because the x-ray and electron data were obtained at different locations. As Imhof et al. noted, the observed x-ray spectrum is consistent with a bremsstrahlung origin.

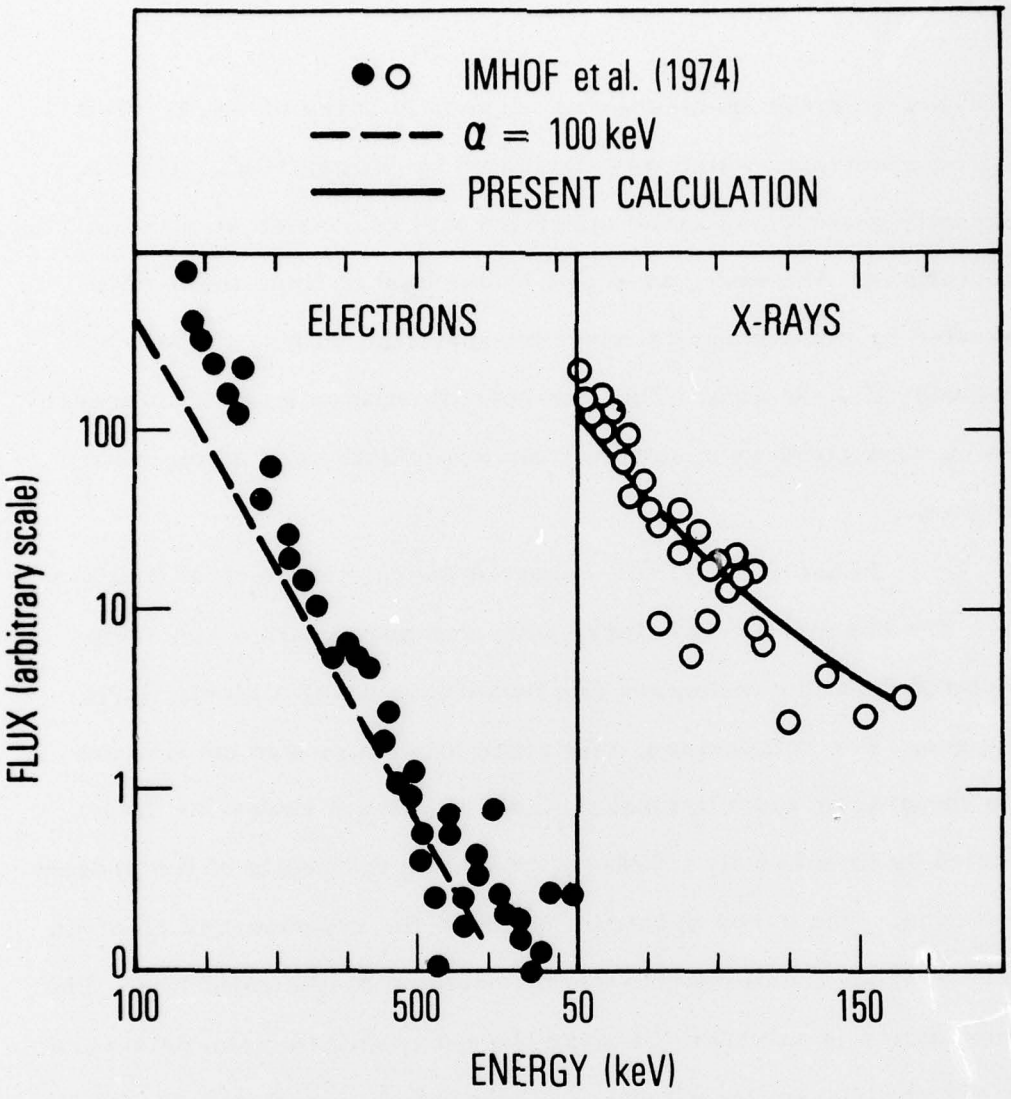

Figure 9. Comparison of Correlated Electron and X-Ray Measurements of Imhof et al. (1974) With the Results of the Present Calculation for an Exponential Electron Spectrum With 100-keV e-Folding Energy

IV. CONCLUDING REMARKS

Estimates of the soft auroral x-ray flux between 0.1 keV and 10 keV have been obtained using a numerical method that produces approximately the same results above 10 keV as Monte Carlo calculations. It was shown that K_α line emission by impact-excited oxygen and nitrogen atoms can increase the auroral x-ray flux below a kilovolt by more than an order of magnitude. Hence, the soft x-rays expected from typical auroral electron precipitation appear to be an ideal medium for auroral imaging from a satellite platform.

REFERENCES

Anderson, K. A.	1965	Auroral Phenomena, ed. by M. Wolt, Stanford University Press, Palo Alto, California 46.
Berger, M. J. and Seltzer, S. M.	1972	J. Atmos. Terr. Phys. 34, 84.
Frank, L. A. and Ackerson, K. L.	1971	J. Geophys. Res. 77, 4116
Hubbell, J. H.	1971	Atomic Data 3, 241
Imhof, W. L.	1975	International Conference on X-rays in Space University of Calgary, Calgary, Alberta, Canada, 741.
Imhof, W. L., Nakano, G. H., Johnson, R. G. and Reagan, J. B.	1974	J. Geophys. Res. 79, 565.
Imhof, W. L., Nakano, G. H., Gaines, E. E. and Reagan, J. B.	1975a	J. Geophys. Res. 80 3622.
Imhof, W. L., Nakano, G. H. and Reagan, J. B.	1975b	J. Geophys. Res. 80 3629.
Jacchia, L. G.	1971	Smithsonian Astrophysical Observatory Special Report 332.
Jones, A. V.	1974	Aurora, Reidel, Dortrecht.

Kremser, G.	1967	Aurora and Airglow, edited by B. M. McCormac, 477.
Kraushaar, W. L.	1974	In Proc. Workshop on Electron Contamination in X-ray Astronomy Experiments, NASA X-661-74-130, Goddard Space Flight Center, Greenbelt, Maryland.
Luhmann, J. G.	1976a	J. Atmos. Terr. Phys., in press.
Luhmann, J. G.	1976b	J. Atmos. Terr. Phys. 38, 605.
Lui, A. T. Y. and Anger C. D.	1973	Planet. Sp. Sci. 21, 799.
Lui, A. T. Y, Anger, C. D. Venkatsan, D., Sawchuk, W. and Akasofu, S. I.	1975	J. Geophys. Res. 80, 1795
Mizera, P. F. Croley, Jr. D. R., Morse, F. A., and Vampola, A. L.	1975	J. Geophys. Res. 80, 2129.
Peterson, L. E.	1975	Instrumental Technique in X-ray Astronomy, Ann. Rev. Astron, Astrophys. 13, 423.
Potemra, T. A. and Zmuda, A. J.	1970	J. Geophys. Res. 75, 7161.
Rees, M. H.	1964	Planet. Space Sci. 12, 1093.
Rogers, E. H., Nelson, D. F., and Savage, R. C.	1974	Science, 183, 951.

Seltzer, S. M. and Berger, M. J.	1974	J. Atmos. Terr. Phys. 36, 1283.
Snyder, A. L., Akasofu, S. I., and Davis, T. N.	1974	J. Geophys. Res. 79, 1393.
Tawara, H., Hsrrison, K. G., and de Heer, F. J.	1973	Physica 63, 351.
Torr, D. G., Torr, M. R., Walker, J. C. G., and Hoffman, R. A.	1975	Planet. Space Sci. 23, 15.
Vij, K. K. and Venkatesan, D.	1975	International Conference on X-rays in Space, University of Calgary, Calgary, Alberta, Canada, 780.
Wilson, B. G., Baxter, A. J., and Green, D. W.	1969	Canadian J. Phys. 47, 2427.

THE IVAN A. GETTING LABORATORIES

The Laboratory Operations of The Aerospace Corporation is conducting experimental and theoretical investigations necessary for the evaluation and application of scientific advances to new military concepts and systems. Versatility and flexibility have been developed to a high degree by the laboratory personnel in dealing with the many problems encountered in the nation's rapidly developing space and missile systems. Expertise in the latest scientific developments is vital to the accomplishment of tasks related to these problems. The laboratories that contribute to this research are:

Aerophysics Laboratory: Launch and reentry aerodynamics, heat transfer, reentry physics, chemical kinetics, structural mechanics, flight dynamics, atmospheric pollution, and high-power gas lasers.

Chemistry and Physics Laboratory: Atmospheric reactions and atmospheric optics, chemical reactions in polluted atmospheres, chemical reactions of excited species in rocket plumes, chemical thermodynamics, plasma and laser-induced reactions, laser chemistry, propulsion chemistry, space vacuum and radiation effects on materials, lubrication and surface phenomena, photosensitive materials and sensors, high precision laser ranging, and the application of physics and chemistry to problems of law enforcement and biomedicine.

Electronics Research Laboratory: Electromagnetic theory, devices, and propagation phenomena, including plasma electromagnetics; quantum electronics, lasers, and electro-optics; communication sciences, applied electronics, semiconducting, superconducting, and crystal device physics, optical and acoustical imaging; atmospheric pollution; millimeter wave and far-infrared technology.

Materials Sciences Laboratory: Development of new materials; metal matrix composites and new forms of carbon; test and evaluation of graphite and ceramics in reentry; spacecraft materials and electronic components in nuclear weapons environment; application of fracture mechanics to stress corrosion and fatigue-induced fractures in structural metals.

Space Sciences Laboratory: Atmospheric and ionospheric physics, radiation from the atmosphere, density and composition of the atmosphere, aurorae and airglow; magnetospheric physics, cosmic rays, generation and propagation of plasma waves in the magnetosphere; solar physics, studies of solar magnetic fields; space astronomy, x-ray astronomy; the effects of nuclear explosions, magnetic storms, and solar activity on the earth's atmosphere, ionosphere, and magnetosphere; the effects of optical, electromagnetic, and particulate radiations in space on space systems.

THE AEROSPACE CORPORATION
El Segundo, California

• • •